

## Prospectively Motion Compensated Amide Proton Transfer MRI for Body Oncology

Jochen Keupp<sup>1</sup>, Guang Jia<sup>2</sup>, Ivan E Dimitrov<sup>3</sup>, Silke Hey<sup>4</sup>, and Michael Knopp<sup>2</sup>

<sup>1</sup>Philips Research, Hamburg, Germany, <sup>2</sup>Department of Radiology, The Ohio State University, Columbus, OH, United States, <sup>3</sup>Philips Healthcare, Cleveland, OH, United States, <sup>4</sup>Philips Healthcare, Best, Netherlands

**Purpose** - In recent years, saturation transfer (ST) MRI techniques based on endogenous contrast of exchangeable amide protons of intracellular proteins and peptides (amide proton transfer, APT)<sup>1</sup> have been developed successfully and applied in first clinical studies for oncology and neurology applications. The work has been mostly focused on applications in the brain<sup>2</sup>, with recent extensions to e.g. prostate<sup>3</sup> and breast<sup>4</sup>. The organs addressed so far are not subject to respiratory motion. Body oncology applications in e.g. liver and kidney are challenging for APT, because the time scale of RF saturation needed for sensitive APT MRI (about 2s) is of the same order as typical respiratory intervals. A basic respiratory triggered ST technique was previously researched for contrast agent studies in human kidneys<sup>5</sup>. In the current work, this approach was extended for improved stability of the contrast with varying respiratory cycles, scan time efficiency and SAR management. The novel technique was tested in human volunteers with a focus on APT contrast in liver and kidney.

**Methods** - Experiments were performed on a clinical MRI system equipped with parallel transmission technology (AchievaTX 3.0T, Philips Healthcare, NL) using a 32-channel torso array-coil for signal reception. Respiratory triggered APT was implemented using continuous pulsed RF saturation (duration  $T_{\text{sat}}$ ) over 1...N respiratory cycles and permanent tracking of the motion state at intervals of 100ms. For SAR management, the maximum saturation time  $T_{\text{max}}$  is pre-defined and monitored. Saturation power is switched off, if  $T_{\text{sat}} > T_{\text{max}}$  for a long respiratory interval (e.g. subject holding breath). In this case, the current k-space segment is not acquired, because the ST contrast would be compromised by switching off saturation prematurely. Instead, a time delay is inserted to settle SAR and saturation is continued afterwards. In the regular case  $T_{\text{sat}} \leq T_{\text{max}}$ , image acquisition is started at the end-expiratory trigger point with a pre-defined delay  $T_d$ . A waiting period  $T_{\text{cool}}$  for SAR cooldown is inserted before the subsequent saturation pulses. The motion state is continuously tracked during the delays ( $T_d$ ,  $T_{\text{cool}}$ ). APT contrast is controlled by defining a minimum saturation time  $T_{\text{min}}$ . If a short respiratory interval is detected that would lead to  $T_{\text{sat}} < T_{\text{min}}$ , pulsed saturation is continued beyond the trigger point and extended into the next respiratory cycle ("cycle extension").

Five healthy volunteers were enrolled, from whom informed consent was obtained. A respiratory belt was applied for motion tracking. A dual-echo 2D segmented GRE sequence was used: FOV 497 mm(LR) $\times$ 200 mm(FH), coronal orientation, matrix 276 $\times$ 122, resolution 1.8 $\times$ 1.8 $\times$ 6 mm<sup>3</sup> (reconstruction 0.8 mm), one respiratory cycle per segment - increased to 2 or more cycles in case of cycle extension, 4 segments per saturation frequency offset, TR=8.5 ms, TE<sub>1</sub>/TE<sub>2</sub>=2.4/5.8 ms,  $\alpha=35^\circ$ , pixel bandwidth 340 Hz, saturation pulse-elements via alternated parallel transmission<sup>6</sup> (50 ms per channel, block shape, amplitudes adapted for equal mean  $B_1$  per channel), 100% duty-cycle,  $B_{1,\text{rms}}=1.8 \mu\text{T}$ , one far off-resonant saturation for normalization ( $S_0$ , -160 ppm) and saturation frequency offsets around  $\Delta\omega=\pm 3.5$  ppm (NH). Specific parameters used for liver APT: 19 saturation frequency offsets in steps of 0.4 ppm,  $T_{\text{max}}=5.2\text{s}$ ,  $T_{\text{min}}=1\text{s}$ ,  $T_d=0.8\text{s}$ ,  $T_{\text{cool}}=1.6\text{s}$ ,  $\approx 7$  min acquisition time (depending on the actual respiratory intervals); kidney APT: 9 frequency offsets, step 0.7 ppm,  $T_{\text{max}}=7\text{s}$ ,  $T_{\text{min}}=1.7\text{s}$ ,  $T_d=0.8\text{s}$ ,  $T_{\text{cool}}=2.7\text{s}$ ,  $\approx 5$  min acquisition. From the dual-echo dataset,  $\delta B_0$  maps were reconstructed for each saturation frequency offset by iterative reconstruction (2-point-Dixon/IDEAL), averaged and used for voxel-wise reconstruction of the  $\delta B_0$ -corrected magnetization transfer asymmetry  $\text{MTR}_{\text{asym}}=(S_{-\Delta\omega}-S_{+\Delta\omega})/S_0$ .

**Results and Discussion** - Prospectively motion compensated APT MRI could be successfully performed in the abdomen achieving stable trigger conditions as well as reproducible quality and trigger position over the different acquired saturation frequency offset images. A liver imaging example is shown in Figure 1. The selected saturation offset ( $\Delta\omega=+3.5\text{ppm}$ , cropped to 320mm in LR direction) displayed in Fig.1a is representative for the achieved image quality as best judged by the sharp representation of the diaphragm. Some artifacts remain due to cardiac pulsation and bowel motion outside the liver. The corresponding  $\text{MTR}_{\text{asym}}$  map is shown in Fig.1b, which exhibits a slightly positive and homogeneous background APT effect in the liver tissue of ( $1.5\pm 1.0\%$ ), except for the major blood vessels, which show larger positive values, likely due to variable flow effects over the different saturation offset images. The diaphragm is sharply imaged with a minor and very narrow asymmetry artifact at the border. An example for APT imaging in the kidneys is shown in Fig.2a (single saturation offset) and 2b ( $\text{MTR}_{\text{asym}}$ ), again providing very sharp delineation of the organs and low asymmetry artifact level due to the stable trigger. While the APT contrast in the renal medulla is low and homogeneous ( $0.5\pm 1.5\%$ ), increased contrast ( $5.5\pm 4\%$ ) is perceived in the left and right renal pelvic areas. The latter is likely originating from urea, with a spectrally broad ST effect of amine groups ( $-\text{NH}_2$ ). The definition of  $T_{\text{min}}$  in combination with automatic cycle extension proves to be an important mechanism to achieve reproducible APT contrast with variable respiration, as in realistic clinical conditions. Variation of  $T_{\text{sat}} > T_{\text{min}}$  due to changing respiration patterns is allowable in case of long RF saturation, because the ST contrast is robust near to complete saturation ( $T_{\text{sat}} \approx 2$  s for amides). In conclusion, stable APT MRI in the abdomen was demonstrated on a clinical MRI scanner using a novel trigger and real-time control mechanism for prospective motion compensation.

**References** - 1. Zhou J et al., Using the amide proton signals of intracellular proteins and peptides to detect pH effects in MRI. Nat Med. 2003; 9(8):1085-90. 2. Wen Z et al., MR imaging of high-grade brain tumors using endogenous protein and peptide-based contrast. Neuroimage. 2010; 51(2):616-22. 3. Jia G et al., Amide proton transfer MR imaging of prostate cancer: a preliminary study. JMIR 2011; 33(3):647-54. 4. Dula AN et al., Amide proton transfer imaging of the breast at 3T. MRM Aug.2012 [Epub] 5. Dimitrov I et al., In vivo human kidney pH mapping at 3T using time-interleaved parallel RF transmission. Proc. ISMRM 20;742 (2012). 6. Keupp J et al., Parallel RF Transmission based MRI Technique for Highly Sensitive Detection of Amide Proton Transfer in the Human Brain at 3T. Proc. ISMRM 19:710 (2011)

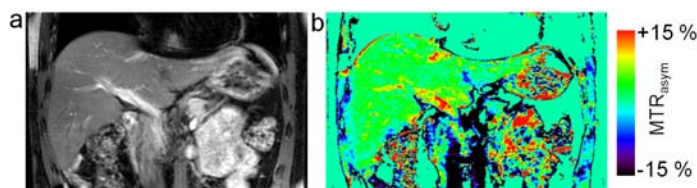


**Figure 1:** Motion compensated liver APT measurement obtained in a healthy volunteer. For a single saturation offset, the liver is imaged with good quality (a).  $\text{MTR}_{\text{asym}}$  of the liver tissue (b) is homogeneously imaged over the entire organ. Some asymmetry artifacts are visible at the major blood vessels.

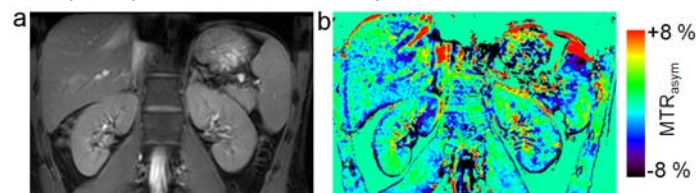


**Figure 2:** APT imaging example on the kidneys (healthy volunteer). The abdominal organs are sharply imaged on the individual saturation offset images (a).  $\text{MTR}_{\text{asym}}$  in the kidney (b) is low and homogeneous in the medulla, but some contrast enhancement is visible in the renal pelvic area, likely due to the ST effect of urea.